

# Electrophilic Addition of $\text{Ph}_3\text{PAu}^+$ to Anionic Alkoxy Fischer-Type Carbene Complexes: A Novel Approach to Metal-Stabilized Bimetallic Vinyl Ether Complexes

Helgard G. Raubenheimer,<sup>\*,†</sup> Matthias W. Esterhuysen,<sup>†</sup> Alexey Timoshkin,<sup>‡</sup> Yu Chen,<sup>‡</sup> and Gernot Frenking<sup>‡</sup>

Department of Chemistry, University of Stellenbosch, Private Bag X1, Matieland, 7602, South Africa, and Fachbereich Chemie, Philipps-Universität Marburg, Hans-Meerwein-Strasse, D-35032 Marburg, Germany

Received January 23, 2002

The addition of the  $\text{Ph}_3\text{PAu}^+$  electrophile to deprotonated Fischer-type alkoxy(methyl)-carbene complexes of pentacarbonyl group 6 metals leads to the formation of novel vinyl ether complexes of gold coordinated to the pentacarbonylmetal moiety. X-ray structures and DFT calculations show that the greatest bonding contribution in the vinyl coordination to the  $\text{M}(\text{CO})_5$  fragment comes from the terminal, partially negatively charged,  $\text{CH}_2$  carbon atom via partial end-on  $\eta^1$ -bonding rather than the usual  $\eta^2$ -bonding of olefins. The corresponding positive charge from the asymmetric vinyl coordination is mainly delocalized onto the  $\text{Ph}_3\text{PAu}$  fragment, stabilizing this coordination mode. The use of W instead of Cr in the  $\text{M}(\text{CO})_5$  fragment, in otherwise isostructural compounds, results in somewhat greater asymmetry in the vinyl coordination, with the difference in the two  $\text{M}(\text{CO})_5$ - $\eta^2$ -vinyl carbon bond lengths increasing from 0.252(11) Å ( $\text{M} = \text{Cr}$ ) to 0.307(5) Å ( $\text{M} = \text{W}$ ) in the solid state.

## Introduction

Since their discovery 38 years ago, Fischer-type carbene complexes and their derivatives have proved their worth as important building blocks and synthons in organic and organometallic synthesis.<sup>1</sup> One unique and extremely useful characteristic of these compounds is that the metal carbonyl moiety serves as a strong electron-withdrawing group, making the protons on groups attached to the carbene carbon highly acidic. This discovery by Kreiter in 1968<sup>2</sup> sparked a plethora of studies involving the addition of electrophiles to the formed conjugate "enolate" anion to yield useful  $\beta$ -substituted carbene complexes (Scheme 1a). Recently Bernasconi et al. determined kinetic and thermodynamic parameters for the carbene deprotonation in acetonitrile/water mixtures.<sup>3</sup> In interpreting the hydrolytic decomposition of  $\beta$ -carbon CH-acidic carbene complexes in a basic medium, weak vinyl ether-Cr(CO)<sub>5</sub>  $\pi$ -complexation, activating the coordinated vinyl ether fragment toward further hydrolysis, is invoked. This alternative conversion (Scheme 1b) is related to the consecutive  $\beta$ -deprotonation, metal reprotonation, and formal reductive elimination of vinyl ethers initiated by weak bases such as pyridine, as first observed by Fischer et al.<sup>4</sup> The formation of  $\alpha$ -stannyl vinyl ethers from the

addition of tributyl tin chloride to the  $\beta$ -deprotonated carbene complex has been reported by McDonald et al. and currently serves as the sole example in which an organometallic vinyl ether is formed along this reaction path.<sup>5</sup> Furthermore, the reverse process, involving the formation of Fischer-type ruthenium carbene complexes from the insertion of  $\pi$ -coordinated vinyl ethers into Ru-H bonds followed by  $\alpha$ -H migration back to Ru, has recently been described.<sup>6</sup> This facile isomerization route to carbene complexes is believed to be enabled by the formation of a stable Ru-H bond and the presence of a  $14e^-$  Ru-complex fragment.

Although the above-mentioned examples highlight the usefulness and synthetic potential of this alternative reaction pathway (Scheme 1b) in carbene chemistry, it is surprising, especially in the light of the amount of research that has been carried out involving carbene anion substitution reactions, that only a handful of conversions following the hydrolytic reaction path are known.<sup>7</sup> Furthermore, nowhere, to our knowledge, have the vinyl ether-M(CO)<sub>5</sub> adducts suggested to form in this reaction been isolated and structurally characterized. We now report the utilization of  $\beta$ -deprotonated carbene complex anions as anionic vinyl synthons, yielding, in a reaction with the  $\text{Ph}_3\text{PAu}^+$  electrophile, unique bimetallic gold(I) vinyl ether-group 6 metal

\* To whom correspondence should be addressed. Fax: +2721 808 3849. Tel: +2721 808 3850. E-mail: hgr@maties.sun.ac.za.

<sup>†</sup> University of Stellenbosch.

<sup>‡</sup> Philipps-Universität Marburg.

(1) For a comprehensive review on the synthetic applications of Fischer carbene complexes see: de Meijere, A.; Schirmer, H.; Duetsch, M. *Angew. Chem., Int. Ed.* **2000**, *39*, 3964, and references therein.

(2) Kreiter, C. G. *Angew. Chem., Int. Ed. Engl.* **1968**, *7*, 390.

(3) Bernasconi, C. F. *Chem. Soc. Rev.* **1997**, *26*, 299.

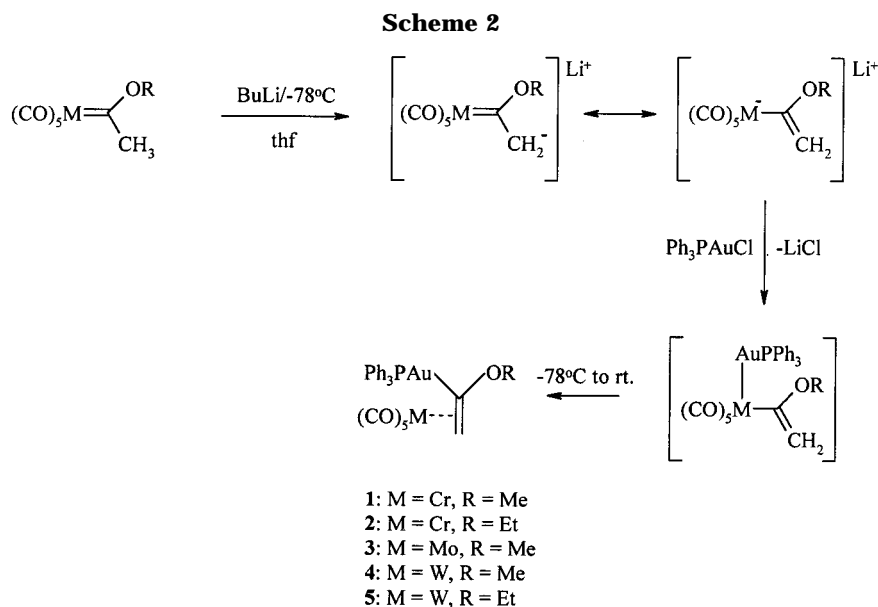
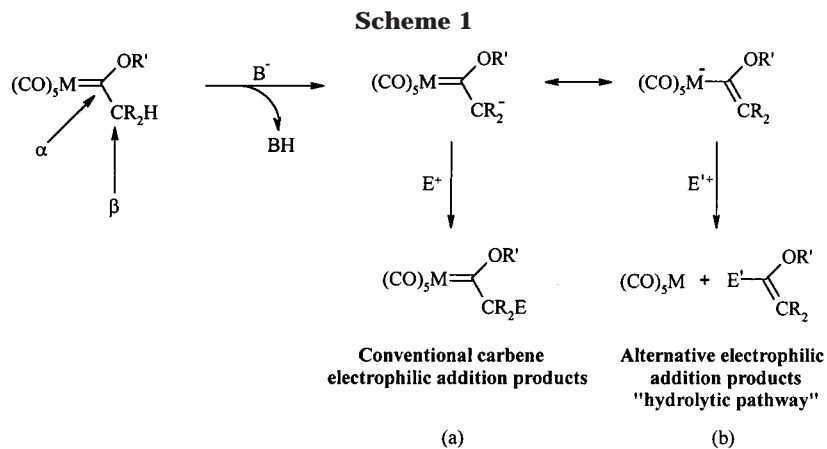
(4) Fischer, E. O.; Plabst, D. *Chem. Ber.* **1974**, *107*, 3326.

(5) McDonald, F. E.; Schultz, C. C.; Chatterjee, A. K. *Organometallics* **1995**, *14*, 3628.

(6) Coalter, J. N., III; Bollinger, J. C.; Huffman, J. C.; Werner-Zwanziger, U.; Caulton, K. G.; Davidson, E. R.; Gérard, H.; Clot, E.; Eisenstein, O. *New J. Chem.* **2000**, *24*, 9.

(7) (a) Fuchibe, K.; Iwasawa, N. *Tetrahedron* **2000**, *56*, 4907. (b) McDonald, F. E.; Reddy, K. S.; Diaz, Y. *J. Am. Chem. Soc.* **2000**, *122*, 4304. (c) Bowman, J. L.; McDonald, F. E. *J. Org. Chem.* **1998**, *63*, 3680.

(d) McDonald, F. E.; Chatterjee, A. K. *Tetrahedron Lett.* **1997**, *38*, 7687.



complexes,  $[M(CO)_5-\{\eta^2\text{-Ph}_3\text{PAu}(\text{OR})=\text{CH}_2\}]$  [ $M = \text{Cr}$ ,  $R = \text{Me}$  (**1**)/ $\text{Et}$  (**2**);  $M = \text{Mo}$ ,  $R = \text{Me}$  (**3**);  $M = \text{W}$ ,  $R = \text{Me}$  (**4**)/ $\text{Et}$  (**5**)]. The synthesis of an uncoordinated  $\alpha$ - $\text{Ph}_3\text{PAu}$  ethyl(vinyl) ether complex by substitution of the  $\text{M}(\text{CO})_5$  metal fragments in **2** and **5** with  $\text{PPh}_3$ , as well as by a transmetalation reaction of  $\alpha$ -ethoxyvinyl lithium with  $\text{Ph}_3\text{PAuCl}$ , is also described. The asymmetric metal  $\pi$ -bonding situation of some of the complexes was, furthermore, analyzed by means of DFT calculations.

## Results and Discussion

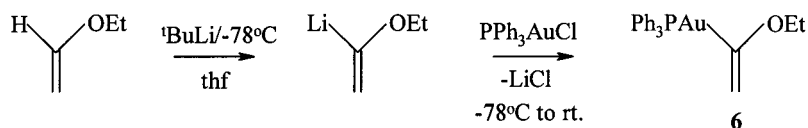
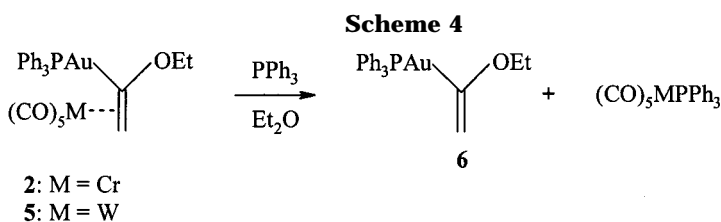
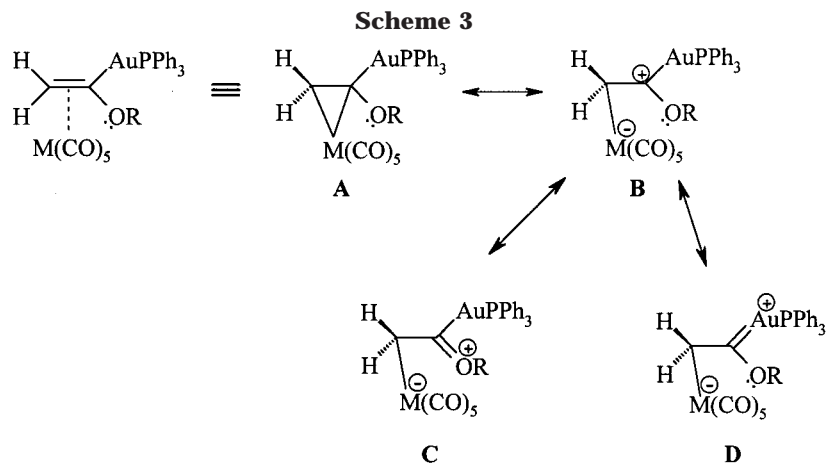
**Electrophilic Addition of the  $\text{Ph}_3\text{PAu}^+$  Fragment to Deprotonated Fischer-Type Alkoxy(methyl)carbene Complexes of Pentacarbonyl Group 6 Metals.** The syntheses of complexes **1–5** (Scheme 2) were carried out in thf at  $-78^\circ\text{C}$ , although some manipulations occurred at room temperature. Product separation of dark yellow to brown, oily reaction mixtures (45–71% yields after separation) was carried out by low-temperature ( $-15^\circ\text{C}$ ) silica gel column chromatography with pentane/diethyl ether (10:1) as eluant, followed by crystallization from a diethyl ether solution layered with pentane at  $-20^\circ\text{C}$ . The reaction is characterized by alkenyl transmetalation and the concomitant, remarkably strong, asymmetric coordination of the vinyl double bond to the  $\text{M}(\text{CO})_5$  fragment.

The formation of  $\eta^2$ -coordinated  $\text{M}(\text{CO})_5$ - $[\text{Ph}_3\text{PAu}$  alkyl(vinyl)ether] bimetallic complexes (**1–5**), via a hydrolysis-type reaction pathway, can, on account of the well-documented and successfully applied isolobal relationship<sup>8</sup> between  $\text{Ph}_3\text{PAu}^+$  and  $\text{H}^+$ , be described as an "aurolysis" reaction. We accept as a working hypothesis formation of the gold vinyl ether complex by sequential auration of the metal carbonyl, formal reductive elimination, and vinyl double-bond coordination to the  $\text{M}(\text{CO})_5$  fragment.

Slippage of the  $\eta^2$ -vinyl coordination toward  $\eta^1$ -coordination in general greatly activates olefin complexes toward nucleophilic addition reactions.<sup>9</sup> Such activation is observed in the complexation of nonmetalated vinyl ethers to group 6  $\text{M}(\text{CO})_5$  fragments and is postulated as a step in the hydrolysis of Fischer carbenes.<sup>3</sup> The coordinated vinyl double bonds are activated toward nucleophilic addition reactions (usually base hydrolysis with  $\text{OH}^-$ ) upon asymmetric coordination. Corresponding aldehyde and alcoholic hydrolysis products are found among decomposition products. Test reactions to prepare gold-free  $\text{M}(\text{CO})_5$ -ethyl(vinyl) ether complexes in neutral media by irradiation of group 6

(8) (a) Hall, K. K.; Mingos, D. M. P. *Prog. Inorg. Chem.* **1984**, 32, 237. (b) Evans, D. G.; Mingos, D. M. P. *J. Organomet. Chem.* **1982**, 232, 171. (c) Hoffmann, R. *Angew. Chem., Int. Ed. Engl.* **1982**, 21, 711.

(9) Eisenstein, O.; Hoffmann, R. *J. Am. Chem. Soc.* **1981**, 103, 4308.



$M(CO)_6$  with UV light in thf followed by addition of ethyl(vinyl) ether also resulted in the formation of a mixture of decomposition and hydrolysis products, including acetaldehyde and ethanol (NMR). When competing ligands ( $L'$ ), e.g., pyridine, are present in the reaction mixture, free vinyl ether and  $M(CO)_5L'$  products can, however, be isolated.<sup>4</sup> In contrast to the above-mentioned findings, activation of the  $M(CO)_5$ -coordinated gold vinyl ethers in complexes **1–5** toward hydrolysis was not observed. In fact, **1–5** are stable in mildly basic or acidic environments and could be purified effectively by silica gel column chromatography. This unique stability of the gold–vinyl ether asymmetric  $\pi$ -complexation can be ascribed to zwitterionic resonance stabilization of the partial positive charge on the  $\alpha$ -vinyl carbon through delocalization to the  $Ph_3PAu$  fragment (structure **D** in Scheme 3;  $Au=C$  double bond is purely illustrative for positive charge delocalization to Au). Evidence for such an assumption is presented in the spectroscopic, computational, and X-ray structure sections.

**Synthesis and Isolation of  $\alpha$ - $Ph_3PAu$  Ethyl(vinyl) Ether (**6**).** To investigate the effects that coordination of the vinyl moiety to the  $M(CO)_5$  groups in **1–5** has on the vinyl ether, the uncoordinated  $\alpha$ - $Ph_3PAu$  ethyl(vinyl) ether complex (**6**) was isolated and characterized. Complex **6** could be obtained in two ways: by freeing the  $\eta^2$ -coordinated  $Ph_3PAu$  ethyl(vinyl) ether units in **2** and **5** with a stronger coordinating ligand (e.g.,  $PPh_3$ ) or by the transmetalation reaction of  $\alpha$ -ethoxyvinyl lithium with  $Ph_3PAuCl$  in thf (Scheme 4).

The substitution reaction was carried out by the addition of  $PPh_3$  to an ether solution of **2** or **5** at  $-15$  °C, after which **6** was purified by column chromatography ( $SiO_2$ ), followed by crystallization from thf layered with pentane at  $-20$  °C (75% yield after separation). In the transmetalation reaction  $\alpha$ -ethoxyvinyl lithium, prepared from  $tBuLi$  and ethyl vinyl ether, was reacted with 1 molar equiv of  $Ph_3PAuCl$  in thf at  $-78$  °C. Complex **6** was mechanically separated in low yield as colorless crystalline needles after crystallization of the reaction mixture from thf/pentane ( $-20$  °C). The balance of crystals consisted mainly of unreacted  $Ph_3PAuCl$  (NMR, TLC).

**Spectroscopic Characterization of **1–6**.** The  $^1H$  NMR spectra of **1–6** (summarized in Table 1) are characterized, in particular, by two distinctive signals, each integrating for a single proton and representing two chemically nonequivalent vinyl protons. For the  $Ph_3PAu$  methyl(vinyl) ether  $\pi$ -complexes of  $Cr(CO)_5$ ,  $Mo(CO)_5$ , and  $W(CO)_5$  (**1**, **3**, and **4**), these signals appear as broadened or doublet resonances at  $\delta$  2.23, 2.66, and 2.73 and doublet resonances at  $\delta$  3.80, 4.26, and 4.17, respectively. The signals at  $\delta$  3.80, 4.26, and 4.17 are assigned to the vinyl protons trans to the  $Ph_3PAu$  fragment coupling with the phosphorus atom across the vinyl group and the gold atom. Although all the signals for the vinyl proton cis to the  $Ph_3PAu$  fragment at  $\delta$  2.23, 2.66, and 2.73 show broadening, a 1.2 Hz  $^4J_{P-H}$  coupling to the phosphorus atom is only observed for the tungsten complex (**4**). No geminal  $^2J_{H-H}$  coupling

**Table 1. Selected NMR Data for Complexes 1–6**

	<sup>1</sup> H <sup>a</sup>		<sup>13</sup> C{ <sup>1</sup> H} <sup>b</sup>		<sup>31</sup> P{ <sup>1</sup> H} <sup>c</sup>
	P–Au–C=CH <sub>cis</sub>	P–Au–C=CH <sub>trans</sub>	P–Au–C=CH <sub>2</sub>	Au–C	Au–P
<b>1</b> <sup>d</sup>	2.23 (br s, 1H)	3.80 (d, <sup>4</sup> J <sub>P–H</sub> = 8.2 Hz, 1H)	56.3 (d, <sup>3</sup> J <sub>P–C</sub> = 8.7 Hz)	191.4 (d, <sup>2</sup> J <sub>P–C</sub> = 124.5 Hz)	41.6 (s)
<b>2</b> <sup>e</sup>	2.16 (br s, 1H)	3.71 (d, <sup>4</sup> J <sub>P–H</sub> = 8.4 Hz, 1H)	55.6 (d, <sup>3</sup> J <sub>P–C</sub> = 8.4 Hz)	192.1 (d, <sup>2</sup> J <sub>P–C</sub> = 120.9 Hz)	41.4 (s)
<b>3</b> <sup>e</sup>	2.66 (br s, 1H)	4.26 (d, <sup>4</sup> J <sub>P–H</sub> = 8.6 Hz, 1H)	61.7 (d, <sup>3</sup> J <sub>P–C</sub> = 6.0 Hz)	186.0 (d, <sup>2</sup> J <sub>P–C</sub> = 134.2 Hz)	40.3 (s)
<b>4</b> <sup>e</sup>	2.73 (d, <sup>4</sup> J <sub>P–H</sub> = 1.2 Hz, 1H)	4.17 (d, <sup>4</sup> J <sub>P–H</sub> = 8.1 Hz, 1H)	57.1 (d, <sup>3</sup> J <sub>P–C</sub> = 9.8 Hz)	185.3 (d, <sup>2</sup> J <sub>P–C</sub> = 124.5 Hz)	40.5 (s)
<b>5</b> <sup>e</sup>	2.71 (d, <sup>4</sup> J <sub>P–H</sub> = 1.7 Hz, 1H)	4.13 (d, <sup>4</sup> J <sub>P–H</sub> = 8.0 Hz, 1H)	56.3 (d, <sup>3</sup> J <sub>P–C</sub> = 9.3 Hz)	185.2 (d, <sup>2</sup> J <sub>P–C</sub> = 121.3 Hz)	40.8 (s)
<b>6</b> <sup>e</sup>	3.76 (br s, 1H)	4.64 (d, <sup>4</sup> J <sub>P–H</sub> = 9.4 Hz, 1H)	94.4 (d, <sup>3</sup> J <sub>P–C</sub> = 6.7 Hz)	202.5 (d, <sup>2</sup> J <sub>P–C</sub> = 129.8 Hz)	42.9 (s)

<sup>a</sup> 600 MHz. <sup>b</sup> 150 MHz. <sup>c</sup> 121.4 MHz. <sup>d</sup> Measured in CDCl<sub>3</sub> at 25 °C. <sup>e</sup> Measured in CD<sub>2</sub>Cl<sub>2</sub> at 25 °C.

between the vinyl protons is observed. The <sup>1</sup>H resonances for the methoxy-CH<sub>3</sub> protons in **1**, **3**, and **4** are found as singlets at δ 3.92, 3.83, and 3.85, roughly 1 ppm upfield from the signals for the same protons in the corresponding methoxy(methyl)carbene starting complexes.<sup>10</sup>

The <sup>13</sup>C{<sup>1</sup>H} NMR signals for the η<sup>2</sup>-coordinated β-vinyl carbons in **1**, **3**, and **4** (Table 1) appear as doublets at δ 56.3, 61.7, and 57.1, while those for the α-vinyl carbons, bonded directly to the Ph<sub>3</sub>PAu fragments, emerge as doublets (<sup>2</sup>J<sub>C–P</sub> = 124.5–134.2 Hz) at δ 191.4, 186.0, and 185.3. The <sup>13</sup>C resonances for the OCH<sub>3</sub> groups in **1**, **3**, and **4** occur at ~δ 61, nearly 10 ppm upfield from the signals for the same resonances in the corresponding metal pentacarbonyl methoxy-(methyl)carbene complexes.<sup>10</sup>

The <sup>1</sup>H NMR spectra of the η<sup>2</sup>-coordinated M(CO)<sub>5</sub>–[Ph<sub>3</sub>PAu ethyl(vinyl) ether] π-complexes [**2** (M = Cr) and **5** (M = W)] are similar to those of **1**, **3**, and **4** with respect to the cis and trans vinyl proton resonances, which appear at δ 2.16 and 2.71 and δ 3.71 and 4.13, respectively. Again, a 1.7 Hz <sup>4</sup>J<sub>P–H</sub> coupling in the broadened doublet signal for the cis vinyl proton is observed only for the tungsten complex (**5**). The <sup>1</sup>H signals for the CH<sub>2</sub> protons in the ethoxy groups in **2** and **5**, however, display a complex doublet of doublets of quartets multiplicity, which is rationalized as follows: The CH<sub>2</sub> protons in the ethoxy groups are diastereotopic, giving rise to separate signals for each proton (δ 4.26 and 4.42 in **2** and δ 4.06 and 4.42 in **5**). The quartet structure exhibited by each of these signals is ascribed to <sup>3</sup>J<sub>H–H</sub> coupling with the terminal CH<sub>3</sub> protons in the ethoxy group. The signals are then further split into doublets by <sup>2</sup>J<sub>H–H</sub> geminal coupling. The <sup>13</sup>C{<sup>1</sup>H} NMR spectra of **2** and **5** compare well to those found for **1**, **3**, and **4**, with the doublet resonances for the η<sup>2</sup>-coordinated α- and β-vinyl carbons appearing at δ 192.1 and 55.6 and δ 185.2 and 56.3, respectively.

The effect of the η<sup>2</sup>-vinyl coordination to the electron-withdrawing M(CO)<sub>5</sub> fragments in **1–5** on the electronic environment of the vinyl group can be observed clearly by comparing the NMR spectra of the free α-Ph<sub>3</sub>PAu ethyl(vinyl) ether fragment (**6**) to those of complexes **1–5**. In the <sup>1</sup>H NMR spectrum of **6** the signal for the cis vinyl proton appears as a broadened singlet at δ 3.76, roughly 1.0–1.5 ppm downfield compared to the same resonances in complexes **1–5**. Similarly, the doublet signal for the trans vinyl proton in **6** at δ 4.64 is roughly 0.5–1.0 ppm downfield from its position in **1–5**. Also, <sup>13</sup>C NMR signals for the free vinyl carbon atoms in **6** lie downfield compared to the coordinated vinyl carbon atoms in complexes **1–5** (δ 94.4 for β-C<sub>vinyl</sub> and δ 202.5

for α-C<sub>vinyl</sub> compared to δ 55.6–61.7 and 185.2–192.1 in **1–5**). Such downfield shifts upon de-coordination of olefins from transition metals are common and can be ascribed to an increase in s-character of the vinyl carbon hybridization (partial sp<sup>3</sup> character in **1–5** to pure sp<sup>2</sup> character in **6**). Furthermore, it was found that this deshielding upon de-coordination of the vinyl ether moieties in complexes **1–5** is much more pronounced for the β-vinyl than for the α-vinyl carbon atom. The <sup>13</sup>C chemical shifts for the β-vinyl carbon atoms, when comparing the <sup>13</sup>C NMR spectrum of the uncoordinated gold vinyl ether complex (**6**) to those of **1–5**, lie between 32.7 and 38.8 ppm downfield compared to downfield shifts of between 10.4 and 17.3 ppm observed for the α-vinyl carbon atom upon vinyl de-coordination. This finding suggests a greater bonding contribution by the β-vinyl carbon atom to the M(CO)<sub>5</sub> fragment, with the α-vinyl carbon atom retaining more of its sp<sup>2</sup> character after coordination.

This interpretation of the NMR spectra is supported by the X-ray structures of **1** and **4**, which show the distinct presence of asymmetric η<sup>2</sup>-vinyl ether coordination modes. For the α-vinyl carbon atom to retain more sp<sup>2</sup> character than the β-vinyl carbon, some π-bonding contribution from either the gold atom or the alkoxy group must occur (as proposed by resonance structures **C** and **D** in Scheme 3). Since the <sup>1</sup>H and <sup>13</sup>C resonances for the alkoxy-CH<sub>3</sub> and -CH<sub>2</sub> atoms appear appreciably upfield compared to their positions in the carbene starting material (in which some double-bond character is ascribed to the C<sub>carbene</sub>–OR bond),<sup>10,11</sup> it can be assumed that delocalization of the partial positive charge on the α-vinyl carbon to the alkoxy fragment is minimal and that the greatest positive charge delocalization takes place to the Ph<sub>3</sub>PAu moiety (resonance structure **D**). This interpretation is strengthened by the <sup>13</sup>C chemical shifts measured for the α-vinyl carbon atom in **1–5** (δ 185.2–192.1), which also support partial carbene character for these atoms,<sup>12</sup> as well as by DFT calculations carried out for the PH<sub>3</sub> analogue of **1**, which report a partial positive charge (+0.28e) situated on the gold atom.

<sup>31</sup>P{<sup>1</sup>H} spectra of **1–5** show singlet signals between 40.3 and 41.6 ppm and are consistent with resonances for PPh<sub>3</sub> on positive or partially positive Ph<sub>3</sub>PAu fragments reported in the literature.<sup>13</sup> Resonance structure **D** is thus suggested as the most important contributing structure to the asymmetry of **1–5**.

(11) Mills, O. S.; Redhouse, A. D. *J. Chem. Soc. (A)* **1968**, 642.

(12) (a) Raubenheimer, H. G.; Desmet, M.; Kruger, G. J. *J. Chem. Soc., Dalton Trans.* **1995**, 2067. (b) Desmet, M.; Raubenheimer, H. G.; Kruger, G. J. *Organometallics* **1997**, *16*, 3324. (c) Raubenheimer, H. G.; Olivier, P. J.; Lindeque, L.; Desmet, M.; Hrušak, J.; Kruger, G. J. *Organomet. Chem.* **1997**, *544*, 91.

(10) Fischer, E. O. *Adv. Organomet. Chem.* **1976**, *14*, 1.

Comparison of the  $^1\text{H}$  and  $^{13}\text{C}$  NMR spectra of **6** to those of nonmetalated ethyl(vinyl) ether shows the effect of substituting the  $\alpha$ -vinyl hydrogen atom with the isolobal  $\text{Ph}_3\text{PAu}$  moiety. Curiously, the  $^1\text{H}$  resonance for the *cis*- $\beta$ -vinyl hydrogen atom appears slightly downfield ( $\delta$  3.94) compared to the corresponding signal in **6** ( $\delta$  3.76), while the signal for the *trans*- $\beta$ -vinyl hydrogen atom appears 0.5 ppm upfield at  $\delta$  4.14. Comparison of the  $^{13}\text{C}$  NMR resonances is more fruitful. The  $\alpha$ - and  $\beta$ -vinyl carbon atoms in ethyl(vinyl) ether resonate at  $\delta$  152.6 and 86.5, compared to  $\delta$  202.5 and 94.4 in complex **6**, indicating greater deshielding of these atoms in **6**. This can be ascribed to electron loss due to  $\sigma$ -donation from the  $\alpha$ -vinyl carbon atom to the  $\text{Ph}_3\text{PAu}$  fragment. The fact that the chemical shift of the  $\beta$ -vinyl carbon atom also indicates slight deshielding upon metalation (7.9 ppm), suggests that  $\pi$ -back-bonding from the gold atom to the  $\pi^*$ -orbitals of the vinyl ether lowering the vinyl bond order and decreasing the  $\pi$ -deshielding effect, is not significant in **6**.

Positive ion FAB-MS of **1–6** exhibited mainly  $\text{Ph}_3\text{PAu}^+$  ( $m/z$  459) and  $(\text{Ph}_3\text{P})_2\text{Au}^+$  ( $m/z$  721) fragments and molecular ions.

The infrared spectra (IR) of **1–5** were recorded in pentane. The  $C_{4v}$ -local metal carbonyl symmetry in **1–5** allows for three IR-active vibrational modes, two  $A_1$  (one with weak intensity) and an intense E mode (a 2-fold degenerate mode). The IR spectra of **1–5** all exhibit five clearly separated absorption bands in the carbonyl region, which could be assigned as follows: one weak  $A_1(1)$  vibrational mode between 2056 and 2064  $\text{cm}^{-1}$ , assigned to the CO symmetric stretching in the  $\text{M}(\text{CO})_4$  plane; a strong  $A_1(2)$  vibrational mode at  $\sim 1910$   $\text{cm}^{-1}$ , assigned to symmetric stretching of the single terminal CO ligand trans to the olefin coordination; a weak  $B_1$  vibrational mode at  $\sim 1976$   $\text{cm}^{-1}$  (IR-active due to distortion of the  $\text{M}(\text{CO})_4$  coordination plane by the large and asymmetric  $\text{Ph}_3\text{PAu}$  vinyl ether ligand), assigned to out-of-plane bending of the CO ligands in the  $\text{M}(\text{CO})_4$  plane. Finally, two strong vibrational modes at  $\sim 1935$  and  $\sim 1924$   $\text{cm}^{-1}$  (due to lifting of E degeneracy) are assigned to the asymmetric stretching of the CO ligands in the  $\text{M}(\text{CO})_4$  plane. Of all these, the  $A_1$  modes have the greatest diagnostic value. Low-frequency  $A_1$  vibrations (compared to literature examples)<sup>14</sup> in complexes of the type  $\text{M}(\text{CO})_5\text{L}$ , as is observed for **1–5** ( $\sim 1910$   $\text{cm}^{-1}$ ), are indicative of good  $\sigma$ -donating, but poor  $\pi$ -accepting ligands (L). This result is also reflected in the small reduction in the vinyl bond order and good retention of  $\text{sp}^2$  geometry found for the coordinating vinyl carbon atoms in the crystal structures of **1** and **4**. Together with the information obtained from the crystal structures of **1** and **4**, the IR spectra of **1–5** suggest that back-donation of electrons from the  $\text{M}(\text{CO})_5$  fragments into the empty  $\pi^*$ -orbitals of the olefins is minimal and that coordination of the vinyl groups into the  $\text{M}(\text{CO})_5$

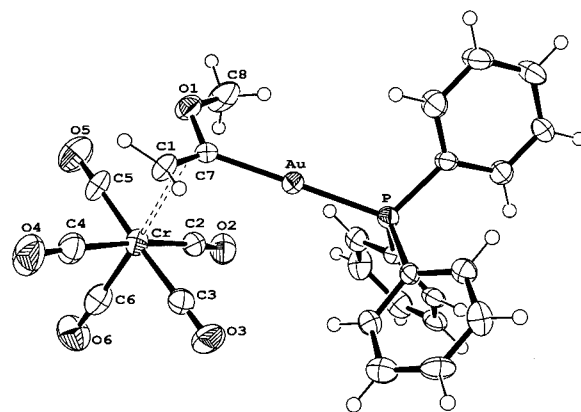


**Figure 1.** ORTEP<sup>18</sup> view of the molecular structure of **1** showing atom-labeling scheme (using 50% probability ellipsoids). Selected interatomic distances (Å) and angles (deg): Au–C(7) = 2.050(7), C(1)–C(7) = 1.345(11), Cr–C(1) = 2.377(8), Cr–C(7) = 2.629(7), C(7)–O(1) = 1.368(9), O(1)–C(8) = 1.424(9), Au–P = 2.291(2), Cr–C(2) = 1.894(9), Cr–C(3) = 1.904(9), Cr–C(4) = 1.885(9), Cr–C(5) = 1.894(10), Cr–C(6) = 1.847(10), Cr–C(1)–C(7) = 85.0(5).

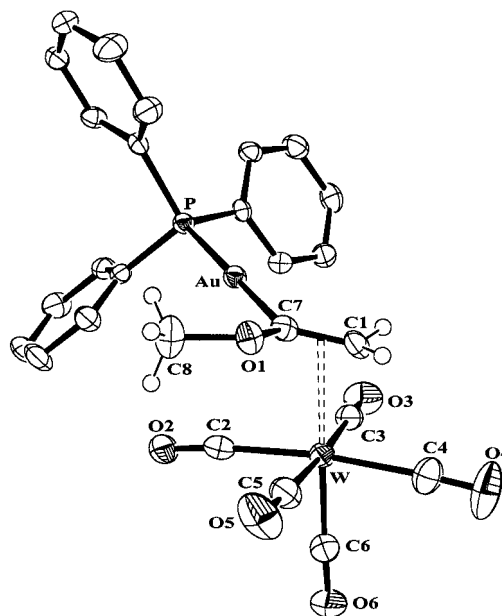


**Figure 2.** ORTEP<sup>18</sup> view of the molecular structure of **4** showing atom-labeling scheme (using 50% probability ellipsoids). Hydrogen atoms on phenyl rings are omitted for clarity. Selected interatomic distances (Å) and angles (deg): Au–C(7) = 2.067(4), C(1)–C(7) = 1.378(5), W–C(1) = 2.393(3), W–C(7) = 2.700(4), C(7)–O(1) = 1.423(4), O(1)–C(8) = 1.436(4), Au–P = 2.294(1), W–C(2) = 2.030(4), W–C(3) = 2.102(4), W–C(4) = 2.048(5), W–C(5) = 2.113(5), W–C(6) = 1.935(4), W–C(1)–C(7) = 87.1(2).

fragments in **1–5** is thus mainly as a result of  $\sigma$ -donation from the olefin. Furthermore, the fact that two clearly separated and nondegenerate vibrational modes (E in  $C_{4v}$  symmetry) are observed bears testimony to the size and asymmetry of the gold alkyl(vinyl) ether ligands.

**X-ray Crystal Structures of 1 and 4.** The crystal and molecular structures of **1** and **4** (Figures 1 and 2) were determined by X-ray diffraction techniques. Both structures show  $\text{Ph}_3\text{PAu}$  methyl vinyl ether moieties coordinated in asymmetrical  $\eta^2$ -fashion to a square

(13) (a) Fernández, E. J.; López-de-Luzuriaga, J. M.; Monge, M.; Olmos, E.; Gimeno, M. C.; Laguna, A.; Jones, P. G. *Inorg. Chem.* **1998**, *37*, 5532. (b) Bayler, A.; Schier, A.; Schmidbauer, H. *Inorg. Chem.* **1998**, *37*, 4353. (c) Chan, W.-H.; Mak, T. C. W.; Che, C.-M. *J. Chem. Soc., Dalton Trans.* **1998**, 2275.

(14) (a) Cotton, F. A.; Kraihanzel, C. S. *J. Am. Chem. Soc.* **1962**, *84*, 4432. (b) Ainscough, E. W.; Brodie, A. M.; Furness, A. R. *J. Chem. Soc., Chem. Commun.* **1971**, 1357. (c) Magee, T. A.; Matthews, C. N.; Wang, T. S.; Wotiz, J. H. *J. Am. Chem. Soc.* **1961**, *83*, 3200. (d) Brown, R. A.; Dobson, G. R. *Inorg. Chim. Acta* **1972**, *6*, 65.

## 1M

pyramidal  $M(\text{CO})_5$  [ $M = \text{Cr}$  (**1**),  $M = \text{W}$  (**4**)] fragment, thus filling the octahedral coordination sphere commonly encountered for group 6 metals in the zero oxidation state. The structures of **1** and **4** represent the first X-ray structures of neutral group 6 metal carbonyl compounds containing vinyl ether ligands. Analysis of the difference in the  $M-\eta^2$  vinyl carbon bond lengths (0.252(11) Å in **1** and 0.307(5) Å in **4**) [ $\Delta(M-C) = \{M-C(7)\} - \{M-C(1)\}$ ] and  $M-C(1)-C(7)$  angles [85.0(5)° and 87.1(2)° in **1** and **4**] gives a clear indication of the asymmetric bonding of the vinyl ethers and shows that the asymmetry is greater in the structure of **4**. Also, the  $M-C(1)$  bond lengths in both structures are very similar [ $\text{Cr}-C(1) = 2.377(8)$  Å,  $\text{W}-C(1) = 2.393(3)$  Å], despite the substantial difference in atomic radius between Cr and W [Cr = 1.25 Å, W = 1.37 Å],<sup>15</sup> illustrating that C(1) is more involved in metal bonding in **4** than in **1**. Slippage of the  $\eta^2$ -vinyl coordination mode toward a  $\eta^1$ -coordination is described by the displacement of the olefin centroid from the metal center (as defined by extension of the  $M-C(6)$  bond). The calculated slip shifts in **1** and **4** (0.00 and 0.04 Å) show that, although the olefin coordination is distinctly asymmetric, no meaningful lateral slippage of the metal toward either vinyl carbon atom has taken place. This is also reflected in the small  $M-C(1)-C(7)$  angles reported above, which are more than 20° from the tetrahedral ideal of 109.5° for pure  $\text{sp}^3$   $\eta^1$ -coordination. In all other known examples where similar asymmetric coordination of an olefin to a metal carbonyl is observed the geometry of the terminal coordinating  $\text{CH}_2$ -carbon atom is much closer to that of an  $\text{sp}^3$  carbon atom and much greater slip shifts are observed.<sup>16</sup>  $C(4)-C(2)-C(7)-C(1)$  torsion angles of 9.4(5)° and 11.3(3)° in **1** and **4** show that the vinyl coordination is close to parallel to the  $C(2)-M-C(4)$  coordination axis in the  $M(\text{CO})_5\text{L}$  octahedra.

Olefin bond lengths [ $C(1)-C(7)$ ] in **1** and **4** of 1.345(11) and 1.378(5) Å compare well to such bonds in known noncoordinated metallo vinyl ethers<sup>17</sup> and indicate that, although formal  $\pi$ -complexation of the vinyl ether has taken place, there is not much reduction in the olefin bond order in the solid state (uncoordinated vinyl ether  $C=C$  bond length in ref 17b is 1.340(5) Å). The geometries of the coordinating vinyl carbon atoms in **1** and **4** are slightly distorted from ideal  $\text{sp}^2$  hybridization, with the greatest deviations from planarity in the mean squares plane defined by  $C(1)$ ,  $C(7)$ ,  $O(1)$ , and Au in **1** and **4** being 0.071(6) and 0.073(3) Å for  $C(7)$  in both cases. The positions of the vinyl protons could be determined from the difference Fourier map and support a slightly distorted  $\text{sp}^2$  hybridization for  $C(1)$  in both structures. These results are in agreement with spectroscopic data for **1** and **4**, which suggest poor back-donation of electrons from the metal to the  $\pi^*$ -orbitals of the olefin, thus conserving the  $\text{sp}^2$  geometry of the coordinated vinyl ether moiety. A slightly greater

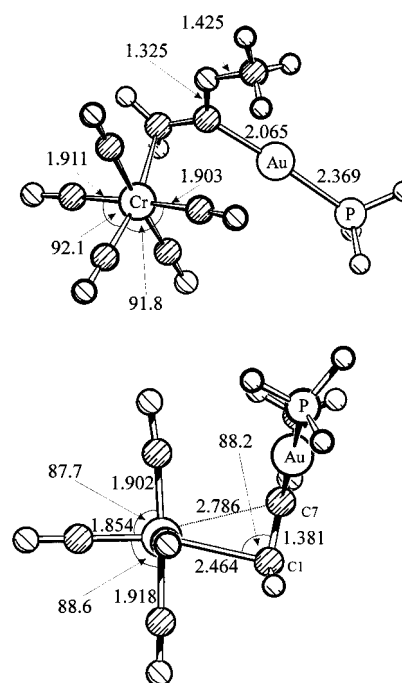


**Figure 3.** Two perspectives of the calculated geometry of **1M**. Distances in Å, angles in deg.

decrease in vinyl bond order and distortion toward  $\text{sp}^3$  geometry is, however, observed in the vinyl bond of **4**.  $\text{Au}-C(7)$  bond lengths in **1** and **4** [2.050(7) and 2.067(4) Å] compare well with literature values in which a gold(I) phosphine fragment is linked via carbon to electron-withdrawing substituents.<sup>19</sup> Furthermore, due to the poor correlation between  $\text{Au}-C$  bond length and bond order,<sup>12</sup> the observed  $\text{Au}-C$  separations do not exclude possible partial carbene character for these bonds, as is suggested by the NMR spectroscopic results and resonance structure **D** (Scheme 3). Reasons for the significant difference in the  $C(7)-O(1)$  bond lengths in **1** and **4** [1.368(9) and 1.432(4) Å] are not clear. Lengths for similar single bonds in noncoordinated metallo vinyl ethers in the literature,<sup>17</sup> however, correlate well with the  $C(7)-O(1)$  separation observed in **1**, suggesting that the  $C(7)-O(1)$  bond in **1** is not shortened, but rather that the  $C(7)-O(1)$  bond in **4** is lengthened. This interpretation thus also supports resonance structure **D** as the main contributing resonance form for these complexes.

Distortion of the  $M(\text{CO})_5$  units due to coordination of the large and asymmetric  $\text{Ph}_3\text{PAu}$  vinyl ether ligand is described by deviation from planarity from the least squares plane through  $M$ ,  $C(2)$ ,  $C(3)$ ,  $C(4)$ , and  $C(5)$  and is calculated as  $-0.071(4)$ ,  $0.049(4)$ ,  $-0.069(4)$ ,  $0.049(4)$ , and  $0.043(3)$  Å in **1** and  $-0.090(2)$ ,  $0.065(2)$ ,  $-0.085(2)$ ,  $0.064(2)$ , and  $0.045(2)$  Å in **4**, respectively.

**DFT Calculations.** To analyze the bonding situation in **1**, we carried out DFT calculations of the model compound **1M** in which the  $\text{PPh}_3$  ligand of **1** is substituted by  $\text{PH}_3$ . Figure 3 shows the optimized geometry

(15) Pauling, L. *The Nature of the Chemical Bond*, 3rd ed.; Cornell University Press: Ithaca, New York, 1960.

(16) Kuhn, N.; Bohnen, H.; Blaser, D.; Boese, R. *Chem. Ber.* **1994**, *127*, 1405.

(17) (a) Baird, G. J.; Davies, S. G.; Jones, R. H.; Prout, K.; Warner, P. *Chem. Commun.* **1984**, 745. (b) Veya, P.; Floriani, C.; Chiesi-Villa, A.; Rizzoli, C. *Organometallics* **1994**, *13*, 214. (c) Xu, D.; Miki, K.; Tanaka, M.; Kasai, N.; Yasuoka, N.; Wada, M. *J. Organomet. Chem.* **1989**, *371*, 267.

(18) Farrugia, L. J. *J. Appl. Crystallogr.* **1997**, *30*, 565.

(19) (a) Steinborn, D.; Becke, S.; Herzog, R.; Gunther, M.; Kircheisen, R.; Stoeckli-Evans, H.; Bruhn, C. Z. *Anorg. Allg. Chem.* **1998**, *624*, 1303. (b) Raubenheimer, H. G.; Kruger, G. J.; Marais, C. F.; Hattingh, J. T. Z.; Linford, L.; van Rooyen, P. H. *J. Organomet. Chem.* **1988**, *355*, 337. (c) Flörke, U.; Haupt, H.-J.; Jones, P. G. *Acta Crystallogr., Sect. C. (Cryst. Struct. Commun.)* **1996**, *52*, 609.

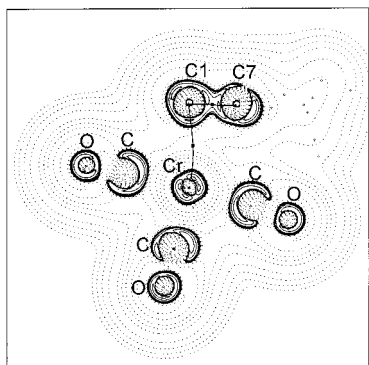


**Figure 4.** Contour line diagrams of the Laplacian distribution  $\nabla^2\rho(\mathbf{r})$  in **1M**. Dashed lines show areas of electron depletion ( $\nabla^2\rho(\mathbf{r}) > 0$ ), while solid lines show areas of electron concentration ( $\nabla^2\rho(\mathbf{r}) < 0$ ). The solid lines between Cr and C1 and between C1 and C7 are the bond paths. There is no bond path between Cr and C7.

and the most important bond lengths and angles of **1M**. The calculated bond lengths and angles of **1M** are very similar to the experimental data of **1**. The theoretical value for the C(1)–C(7) distance is 1.381 Å, which is slightly longer than experiment. More important are the Cr–C bond lengths of the coordinated vinyl group. The calculations also give rather different distances for C(1)–Cr = 2.464 Å and C(7)–Cr = 2.786 Å, indicating stronger bonding of chromium with C(1) than with C(7). A topological analysis of the electron density distribution<sup>20</sup> suggests that the Cr–vinyl bonding takes place mainly via carbon atom C(1) of the ligand. The Laplacian distribution of **1M**, which is given in Figure 4, shows that the area of  $\pi$ -charge concentration at the terminal C(1) atom of the vinyl ether ligand is distorted toward the chromium atom. There is a droplet-like appendix of charge concentration which points toward Cr. Even more revealing concerning the bonding situation are the calculated bond paths. Figure 4 shows that there is a bond path between C(1) and Cr but not between C(7) and Cr. The shape of the Laplacian distribution and the calculated bond paths show clearly that the chromium atom is primarily bonded to C(1) and that there are only secondary interactions between C(7) and Cr. The calculated charge distribution given by the NBO analysis<sup>21</sup> gives a large negative partial charge at C(1) ( $-0.61e$ ) but a small positive charge at C(7) ( $+0.03e$ ). Positive partial charges are also calculated for Au ( $+0.28e$ ) and the  $\text{PH}_3$  ligand ( $+0.23e$ ). This means that the positive charge is delocalized over the C(7)–Au– $\text{PH}_3$  moiety. Despite the charge distribution, however, the calculations give a nearly planar arrangement of the vinyl moiety. We conclude that the bonding interaction between the coordinating vinyl ligand and chromium in **1M** and **1** is best described as  $\eta^1$ -bonding of a terminal carbanion rather than  $\eta^2$ -bonding of an olefin.

The vinyl ether ligand might also bind to the  $\text{M}(\text{CO})_5$  moiety via the oxygen atom of the ether group. We also calculated the isomer of **1M** where the ligand is bonded to chromium through the oxygen atom rather than the

vinyl group (**1M'**). The calculations predict that this isomer is 5.7 kcal/mol higher in energy than **1M**. The negatively charged terminal carbon atom is softer than oxygen and is, thus, a better donor. We also calculated the related isomers where oxygen is substituted by sulfur. The DFT calculations predict that the vinyl thioether ligand binds stronger through the sulfur atom than through the vinyl group. The former isomer is 6.6 kcal/mol lower in energy than the latter. This means that the relative stability of the isomers **1M** and **1M'** changes when oxygen is substituted by sulfur. We are investigating this theoretical prediction.

### Summary

In this paper we have reported the synthesis of asymmetrically coordinated yet stable vinyl ether complexes of group 6 metal pentacarbonyls via an aurolysis reaction of  $\beta$ -carbon deprotonated alkoxy Fischer-type carbene anions with the  $\text{Ph}_3\text{PAu}^+$  electrophile. Evidence presented here strongly suggests that the asymmetric vinyl coordination observed in the structures of these compounds is stabilized by the delocalization of partial positive charges in the polarized vinyl coordination mode to the  $\text{Ph}_3\text{PAu}$  moiety. This effectively allows the isolation of the vinyl ether coordinated complex that has been proposed as a transition state in the hydrolysis of conventional methyl alkoxy Fischer-type carbene complexes. Nowhere, to our knowledge, have such vinyl ether– $\text{M}(\text{CO})_5$  adducts from this reaction been isolated and structurally characterized. Quantum chemical calculations show that the bonding between the chromium atom and the vinyl moiety of the vinyl ether ligand should be considered as  $\eta^1$ -bonding of the terminal carbanion rather than  $\eta^2$ -bonding of an olefin. The isolation of these compounds, furthermore, confirms this reaction pathway as the one by which the hydrolytic decomposition of Fischer carbene complexes takes place. This reaction also serves as a novel and effective method for the preparation of gold vinyl ethers. Currently we are investigating the use of this type of conversion for the preparation of the first gold vinylamines and mercapto vinyl ethers.

### Experimental Section

All procedures were carried out under a dry nitrogen atmosphere using standard Schlenk and vacuum-line techniques. All solvents were dried and purified by conventional methods and freshly distilled under nitrogen shortly before use. Unless otherwise stated all common reagents were used as obtained from commercial suppliers without further purification. Ethyl(vinyl) ether was distilled under nitrogen gas before use. NMR spectra were recorded on Varian INOVA 600 (600 MHz for  $^1\text{H}$ , 151 MHz for  $^{13}\text{C}\{^1\text{H}\}$ , and 243 MHz for  $^{31}\text{P}\{^1\text{H}\}$ ) or Varian VXR 300 (300 MHz for  $^1\text{H}$ , 75.4 MHz for  $^{13}\text{C}\{^1\text{H}\}$ , and 121.5 MHz for  $^{31}\text{P}\{^1\text{H}\}$ ) NMR spectrometers.  $^1\text{H}$  and  $^{13}\text{C}$  chemical shifts are reported in ppm relative to the  $^1\text{H}$  and  $^{13}\text{C}$  residue of the deuterated solvents.  $^{31}\text{P}$  chemical shifts are reported in ppm relative to an 85%  $\text{H}_3\text{PO}_4$  external standard solution. IR spectra were recorded on a Perkin-Elmer 1600 series FTIR spectrometer. FAB-MS were recorded on a Micromass DG 70/70E mass spectrometer using xenon gas as bombardment atoms and *m*-nitrobenzyl alcohol as matrix. Flash column chromatography was performed with "flash grade" silica (SDS 230–400 mesh).

**Representative Experimental Procedures for the Synthesis of 1–5.**  $^n\text{BuLi}$  (0.5 mL, 1.6 M, 1.2 equiv) was added to

(20) Bader, R. F. W. *Atoms in Molecules: A Quantum Theory*; Clarendon Press: Oxford, 1990.

(21) Reed, A. E.; Curtiss, L. A.; Weinhold F. *Chem. Rev.* **1988**, *88*, 899.

**Table 2. Crystallographic Data for 1 and 4**

	<b>1</b>	<b>4</b>
chemical formula	C <sub>26</sub> H <sub>20</sub> O <sub>6</sub> PAuCr	C <sub>26</sub> H <sub>20</sub> O <sub>6</sub> PAuW
MW (g/mol)	708.36	840.21
cryst syst	monoclinic	monoclinic
space group	<i>P</i> 2 <sub>1</sub> / <i>c</i>	<i>P</i> 2 <sub>1</sub> / <i>c</i>
<i>a</i> (Å)	10.6147(4)	10.698(1)
<i>b</i> (Å)	12.0314(4)	12.106(1)
<i>c</i> (Å)	20.4580(9)	20.352(1)
$\alpha$ (deg)	90	90
$\beta$ (deg)	99.705(2)	94.423(1)
$\gamma$ (deg)	90	90
volume (Å <sup>3</sup> )	2575.3(2)	2627.9(4)
<i>Z</i>	4	4
<i>d</i> <sub>calcd</sub> (g/cm <sup>3</sup> )	1.827	2.124
temp (K)	173(2)	150(2)
$\mu_{\text{Mo K}\alpha}$ (cm <sup>-1</sup> )	6.212	10.048
$2\theta_{\text{max}}$ (deg)	25.49	27.00
radiation	Mo K $\alpha$ , graphite monochromated	Mo K $\alpha$ , graphite monochromated
cryst size (mm)	0.012 $\times$ 0.02 $\times$ 0.15	0.13 $\times$ 0.25 $\times$ 0.25
index range	-12 $\leq h \leq$ 12 -14 $\leq k \leq$ 12 -20 $\leq l \leq$ 24	-13 $\leq h \leq$ 10 -15 $\leq k \leq$ 14 -26 $\leq l \leq$ 22
no. of reflns collected	12 767	13 102
no. of ind reflns	4787 ( <i>R</i> <sub>int</sub> = 0.0880)	5627 ( <i>R</i> <sub>int</sub> = 0.0272)
no. of obsd reflns	3158	4872
refinement	SHELXL on <i>F</i> <sup>2</sup>	SHELXL on <i>F</i> <sup>2</sup>
params	325	326
<i>R</i> <sub>1</sub> ( <i>F</i> <sub>o</sub> > 2 $\sigma$ <i>F</i> <sub>o</sub> )	0.0454	0.0219
<i>wR</i> <sub>2</sub> (all data)	0.0867	0.0461

a solution of the alkoxy(methyl) carbene complex (0.8 mmol) in 15 mL of thf cooled to -78 °C. The mixture was stirred at that temperature for 30 min, after which 1 equiv of Ph<sub>3</sub>PAuCl (395 mg) or Ph<sub>3</sub>PAuNO<sub>3</sub> (417 mg) was added to the solution. The mixture was then allowed to warm to room temperature over a period of 3 h. Removal of the solvent in vacuo resulted in dark yellow to brown oily residues containing a mixture of products (TLC). The products were isolated in moderate yields (67% (**1**), 71% (**2**), 53% (**3**), 45% (**4**), and 63% (**5**)) as broad yellow bands by means of low-temperature (-15 °C) silica gel column chromatography (pentane/diethyl ether, 10:1).

**Synthesis of 6: Substitution Reaction.** PPh<sub>3</sub> (1 equiv, 0.05 mmol, 131 mg) was added to a cooled (-15 °C) ether solution of **2** or **5** (0.5 mmol). The mixture was allowed to warm to room temperature over a period of 30 min. Removal of the solvent in vacuo resulted in a powdery, light yellow mixture containing **6** and (CO)<sub>5</sub>MPPH<sub>3</sub> (vide-NMR). **6** was purified by low-temperature (-15 °C) flash silica gel column chromatography (thf/pentane, 1:2), followed by crystallization from thf layered with pentane at -20 °C (75% yield after separation).

**Transmetalation Reaction.** A solution of  $\alpha$ -ethoxyvinyl-lithium (0.8 mmol) in 15 mL of thf was prepared analogously to the procedure for the preparation of  $\alpha$ -methoxyvinyl-lithium described by Baldwin et al.<sup>22</sup> While stirring this solution at -78 °C, 1 equiv of Ph<sub>3</sub>PAuCl (0.8 mmol, 395 mg) was added, after which it was allowed to warm to room temperature over a period of 3 h. Removal of the solvent in vacuo resulted in milky oily residues containing the product and unreacted Ph<sub>3</sub>PAuCl. Complex **6** was isolated as needles in low yield (9%) by crystallization from thf/pentane mixtures at -20 °C. Yields were not optimized.

**X-ray Crystallography.** The crystal and refinement data for **1** and **4** are summarized in Table 2. X-ray quality yellow platelet single crystals of **1** and **4** were obtained by crystallization from concentrated diethyl ether solutions layered with pentane at -20 °C. Data were collected on an Enraf-Nonius KappaCCD diffractometer using graphite-monochromated Mo K $\alpha$  radiation ( $\lambda = 0.71073$  Å) and scaled and reduced using

(22) Baldwin, J. E.; Höfle, G. A.; Lever, O. W., Jr. *J. Am. Chem. Soc.* **1974**, *96*, 7125.

DENZO-SMN.<sup>23</sup> The structures were solved by the heavy atom method (SHELXS)<sup>24</sup> and refined anisotropically for non-hydrogen atoms by full-matrix least squares calculations (SHELXL-97)<sup>24</sup> on *F*<sup>2</sup>. All hydrogen atoms in **1** and **4** were placed in calculated positions, except those on the coordinating vinyl moiety, which were found on the difference Fourier map and refined isotropically.

**Theoretical Calculations.** The geometries have been optimized at the gradient-corrected DFT level using the three-parameter fit of the exchange-correlation potential suggested by Becke<sup>25</sup> in conjunction with the LYP<sup>26</sup> exchange potential (B3LYP).<sup>27</sup> A quasi-relativistic small-core ECP with a (441/2111/N1) valence basis set for the metal atoms (*N* = 4 for Cr and *N* = 2 for Au)<sup>28</sup> and 6-31G(d) all-electron basis sets<sup>29</sup> for the other atoms have been employed in the geometry optimizations. This is our standard basis set II.<sup>30</sup> The nature of the stationary points was examined by calculating the Hessian matrix at B3LYP/II. All structures are energy minima on the potential energy surface. The calculations have been performed with the program package Gaussian 98.<sup>31</sup> The topological analysis of the electron density distribution was carried out with the programs SADDLE, GRID, SCHUSS, CPLOT, and BADERCAT.<sup>32</sup>

**Spectroscopic data for 1:** <sup>1</sup>H NMR (600 MHz, CDCl<sub>3</sub>, 298 K)  $\delta$  2.23 (br s, 1H, *cis*-C=CH<sub>2</sub>), 3.80 (d, <sup>4</sup>*J*<sub>trans P-H</sub> = 8.2 Hz, 1H, *trans*-C=CH<sub>2</sub>), 3.92 (s, 3H, OCH<sub>3</sub>), 7.4–7.6 (m, 15H, Ph); <sup>13</sup>C{<sup>1</sup>H} NMR (150 MHz, CDCl<sub>3</sub>, 298 K)  $\delta$  56.3 (d, <sup>3</sup>*J*<sub>P-C</sub> = 8.7 Hz, =CH<sub>2</sub>), 61.3 (s, OCH<sub>3</sub>), 129.7 (d, <sup>2</sup>*J*<sub>P-C</sub> = 10.9 Hz, *ortho*-Ph), 130.1 (d, <sup>1</sup>*J*<sub>P-C</sub> = 53.4 Hz, *ipso*-Ph), 132.1 (s, *para*-Ph), 134.6 (d, <sup>3</sup>*J*<sub>P-C</sub> = 13.6 Hz, *meta*-Ph), 191.4 (d, <sup>2</sup>*J*<sub>P-C</sub> = 124.5 Hz, C–Au), 219.5 (s, *cis*-CO), 227.2 (s, *trans*-CO); <sup>31</sup>P{<sup>1</sup>H} NMR (243 MHz, CDCl<sub>3</sub>, 298 K)  $\delta$  41.6 (s, PPh<sub>3</sub>); positive ion FAB-MS *m/z* 708 (M<sup>+</sup>); IR (cm<sup>-1</sup>, pentane solution in NaCl cell)  $\nu$ (CO) 1910 (s, A<sub>1</sub>(2)), 1924, 1938 (2  $\times$  s, "E"), 1978 (w, B<sub>1</sub>), 2057 (w, A<sub>1</sub>(1)). Anal. Calcd for C<sub>26</sub>H<sub>20</sub>O<sub>6</sub>PCrAu: C, 44.08; H, 2.85; O, 13.55. Found: C, 44.25; H, 2.98; O, 13.26.

**Spectroscopic data for 2:** <sup>1</sup>H NMR (600 MHz, CD<sub>2</sub>Cl<sub>2</sub>, 298 K)  $\delta$  1.22 (t, <sup>3</sup>*J*<sub>H-H</sub> = 7.1 Hz, 3H, CH<sub>3</sub>), 2.16 (br s, 1H, *cis*-C=CH<sub>2</sub>), 3.71 (d, <sup>4</sup>*J*<sub>trans P-H</sub> = 8.4 Hz, 1H, *trans*-C=CH<sub>2</sub>), 4.26 (dq, <sup>2</sup>*J*<sub>H-H</sub> = 10.0 Hz, <sup>3</sup>*J*<sub>H-H</sub> = 7.1 Hz, 1H, OCH<sub>2</sub>), 4.42 (dq, <sup>2</sup>*J*<sub>H-H</sub> = 10.0 Hz, <sup>3</sup>*J*<sub>H-H</sub> = 7.1 Hz, 1H, OCH<sub>2</sub>), 7.4–7.7 (m, 15H, Ph); <sup>13</sup>C{<sup>1</sup>H} NMR (150 MHz, CD<sub>2</sub>Cl<sub>2</sub>, 298 K)  $\delta$  15.1 (s, CH<sub>3</sub>), 55.6 (d, <sup>3</sup>*J*<sub>P-C</sub> = 8.4 Hz, =CH<sub>2</sub>), 70.6 (s, OCH<sub>2</sub>), 129.6 (d, <sup>2</sup>*J*<sub>P-C</sub> = 11.7 Hz, *ortho*-Ph), 130.0 (d, <sup>1</sup>*J*<sub>P-C</sub> = 53.7 Hz, *ipso*-

(23) Otwinowski, Z.; Minor, W. *Methods Enzymol.* **1997**, *276*, 307.  
(24) Sheldrick, G. M. *SHELX-97*. Program for crystal structure analysis; University of Göttingen: Germany, 1997.

(25) Becke, A. D. *J. Chem. Phys.* **1993**, *98*, 5648.

(26) Lee, C.; Yang, W.; Parr, R. G. *Phys. Rev. B* **1988**, *37*, 785.

(27) Stevens, P. J.; Devlin, F. J.; Chabowski, C. F.; Frisch, M. J. *J. Phys. Chem.* **1994**, *98*, 11623.

(28) Hay, P. J.; Wadt, W. R. *J. Chem. Phys.* **1985**, *82*, 299.

(29) (a) Ditchfield, R.; Hehre, W. J.; Pople, J. A. *J. Chem. Phys.* **1971**, *54*, 724. (b) Hehre, W. J.; Ditchfield, R.; Pople, J. A. *J. Chem. Phys.* **1972**, *56*, 2257.

(30) Frenking, G.; Antes, I.; Böhme, M.; Dapprich, S.; Ehlers, A. W.; Jonas, V.; Neuhaus, A.; Otto, M.; Stegmann, R.; Veldkamp, A.; Vydroshchikov, S. F. In *Reviews in Computational Chemistry*; Lipkowitz, K. B., Boyd, D. B., Eds.; VCH: New York, 1996; Vol. 8, pp 63–144.

(31) Frisch, M. J.; Trucks, G. W.; Schlegel, H. B.; Scuseria, G. E.; Robb, M. A.; Cheeseman, J. R.; Zakrzewski, V. G.; Montgomery, J. A., Jr.; Stratmann, R. E.; Burant, J. C.; Dapprich, S.; Millam, J. M.; Daniels, A. D.; Kudin, K. N.; Strain, M. C.; Farkas, O.; Tomasi, J.; Barone, V.; Cossi, M.; Cammi, R.; Mennucci, B.; Pomelli, C.; Adamo, C.; Clifford, S.; Ochterski, J.; Petersson, G. A.; Ayala, P. Y.; Cui, Q.; Morokuma, K.; Malick, D. K.; Rabuck, A. D.; Raghavachari, K.; Foresman, J. B.; Cioslowski, J.; Ortiz, J. V.; Stefanov, B. B.; Liu, G.; Liashenko, A.; Piskorz, P.; Komaromi, I.; Gomperts, R.; Martin, R. L.; Fox, D. J.; Keith, T.; Al-Laham, M. A.; Peng, C. Y.; Nanayakkara, A.; Gonzalez, C.; Challacombe, M.; Gill, P. M. W.; Johnson, B. G.; Chen, W.; Wong, M. W.; Andres, J. L.; Head-Gordon, M.; Replogle, E. S.; Pople, J. A. *Gaussian 98*, revision A.8; Gaussian, Inc.: Pittsburgh, PA, 1998.

(32) Biegler-König, F. W.; Bader, R. F. W.; Ting-Hua, T. J. *J. Comput. Chem.* **1982**, *3*, 317.



Ph), 131.9 (s, *para*-Ph), 134.5 (d,  $^3J_{P-C} = 12.4$  Hz, *meta*-Ph), 192.1 (d,  $^2J_{P-C} = 120.9$  Hz, C–Au), 219.3 (s, *cis*-CO), 227.0 (s, *trans*-CO);  $^{31}P\{^1H\}$  NMR (243 MHz,  $CD_2Cl_2$ , 298 K)  $\delta$  41.4 (s, PPh<sub>3</sub>); positive ion FAB-MS  $m/z$  722 ( $M^+$ ); IR ( $cm^{-1}$ , pentane solution in NaCl cell)  $\nu(CO)$  1910 (s, A<sub>1</sub>(2)), 1923, 1938 ( $2 \times$  s, "E"), 1978 (w, B<sub>1</sub>), 2056 (w, A<sub>1</sub>(1)). Anal. Calcd for  $C_{27}H_{22}O_6$ -PCrAu: C, 44.89; H, 3.07; O, 13.29. Found: C, 45.12; H, 3.02; O, 13.38.

**Spectroscopic data for 3:**  $^1H$  NMR (600 MHz,  $CD_2Cl_2$ , 298 K)  $\delta$  2.66 (br s, 1H, *cis*-C=CH<sub>2</sub>), 3.83 (s, 3H, OCH<sub>3</sub>), 4.26 (d,  $^4J_{trans\ P-H} = 8.6$  Hz, 1H, *trans*-C=CH<sub>2</sub>), 7.4–7.7 (m, 15H, Ph);  $^{13}C\{^1H\}$  NMR (150 MHz,  $CD_2Cl_2$ , 298 K)  $\delta$  61.1 (s, OCH<sub>3</sub>), 61.7 (d,  $^3J_{P-C} = 6.0$  Hz, =CH<sub>2</sub>), 129.5 (d,  $^2J_{P-C} = 12.0$  Hz, *ortho*-Ph), 130.1 (d,  $^1J_{P-C} = 54.0$  Hz, *ipso*-Ph), 131.9 (s, *para*-Ph), 134.4 (d,  $^3J_{P-C} = 14.5$  Hz, *meta*-Ph), 186.0 (d,  $^2J_{P-C} = 134.2$  Hz, C–Au), 201.5 (s, *cis*-CO), 206.1 (s, *trans*-CO);  $^{31}P\{^1H\}$  NMR (121.4 MHz,  $CD_2Cl_2$ , 298 K)  $\delta$  40.3 (s, PPh<sub>3</sub>); positive ion FAB-MS  $m/z$  752 ( $M^+$ ); IR ( $cm^{-1}$ , pentane solution in NaCl cell)  $\nu(CO)$  1910 (s, A<sub>1</sub>(2)), 1925, 1934 ( $2 \times$  s, "E"), 1980 (w, B<sub>1</sub>), 2060 (w, A<sub>1</sub>(1)). Anal. Calcd for  $C_{26}H_{20}O_6PMoAu$ : C, 41.51; H, 2.68; O, 12.76. Found: C, 41.45; H, 2.64; O, 12.90.

**Spectroscopic data for 4:**  $^1H$  NMR (600 MHz,  $CD_2Cl_2$ , 298 K)  $\delta$  2.73 (d,  $^4J_{cis\ P-H} = 1.2$  Hz, 1H, *cis*-C=CH<sub>2</sub>), 3.85 (s, 3H, OCH<sub>3</sub>), 4.17 (d,  $^4J_{trans\ P-H} = 8.1$  Hz, 1H, *trans*-C=CH<sub>2</sub>), 7.4–7.7 (m, 15H, Ph);  $^{13}C\{^1H\}$  NMR (150 MHz,  $CD_2Cl_2$ , 298 K)  $\delta$  57.1 (d,  $^3J_{P-C} = 9.8$  Hz, =CH<sub>2</sub>), 61.6 (s, OCH<sub>3</sub>), 129.6 (d,  $^2J_{P-C} = 12.2$  Hz, *ortho*-Ph), 130.0 (d,  $^1J_{P-C} = 53.7$  Hz, *ipso*-Ph), 131.9 (s, *para*-Ph), 134.5 (d,  $^3J_{P-C} = 14.6$  Hz, *meta*-Ph), 185.3 (d,  $^2J_{P-C} = 124.5$  Hz, C–Au), 200.1 (s, *cis*-CO), 204.1 (s, *trans*-CO);  $^{31}P\{^1H\}$  NMR (121.4 MHz,  $CD_2Cl_2$ , 298 K)  $\delta$  40.5 (s, PPh<sub>3</sub>); positive ion FAB-MS  $m/z$  840 ( $M^+$ ); IR ( $cm^{-1}$ , pentane solution in NaCl cell)  $\nu(CO)$  1910 (s, A<sub>1</sub>(2)), 1924, 1936 ( $2 \times$  s, "E"), 1976 (w, B<sub>1</sub>), 2064 (w, A<sub>1</sub>(1)). Anal. Calcd for  $C_{26}H_{20}O_6$ -PWAu: C, 37.17; H, 2.40; O, 11.42. Found: C, 37.35; H, 2.62; O, 11.53.

**Spectroscopic data for 5:**  $^1H$  NMR (600 MHz,  $CD_2Cl_2$ , 298 K)  $\delta$  1.25 (t,  $^3J_{H-H} = 7.1$  Hz, 3H, CH<sub>3</sub>), 2.71 (d,  $^4J_{cis\ P-H} = 1.7$  Hz, 1H, *cis*-C=CH<sub>2</sub>), 4.13 (d,  $^4J_{trans\ P-H} = 8.0$  Hz, 1H, *trans*-C=CH<sub>2</sub>), 4.06 (dq,  $^2J_{H-H} = 9.5$  Hz,  $^3J_{H-H} = 7.1$  Hz, 1H, OCH<sub>2</sub>),

4.42 (dq,  $^2J_{H-H} = 9.5$  Hz,  $^3J_{H-H} = 7.1$  Hz, 1H, OCH<sub>2</sub>), 7.4–7.7 (m, 15H, Ph);  $^{13}C\{^1H\}$  NMR (150 MHz,  $CD_2Cl_2$ , 298 K)  $\delta$  15.0 (s, CH<sub>3</sub>), 56.3 (d,  $^3J_{P-C} = 9.3$  Hz, =CH<sub>2</sub>), 70.3 (s, OCH<sub>2</sub>), 129.5 (d,  $^2J_{P-C} = 12.4$  Hz, *ortho*-Ph), 130.7 (d,  $^1J_{P-C} = 47.8$  Hz, *ipso*-Ph), 131.9 (s, *para*-Ph), 134.5 (d,  $^3J_{P-C} = 12.9$  Hz, *meta*-Ph), 185.2 (d,  $^2J_{P-C} = 121.3$  Hz, C–Au), 200.3 (s, *cis*-CO), 204.3 (s, *trans*-CO);  $^{31}P\{^1H\}$  NMR (121.4 MHz,  $CD_2Cl_2$ , 298 K)  $\delta$  40.8 (s, PPh<sub>3</sub>); positive ion FAB-MS  $m/z$  854 ( $M^+$ ); IR ( $cm^{-1}$ , pentane solution in NaCl cell)  $\nu(CO)$  1910 (s, A<sub>1</sub>(2)), 1924, 1935 ( $2 \times$  s, "E"), 1976 (w, B<sub>1</sub>), 2064 (w, A<sub>1</sub>(1)). Anal. Calcd for  $C_{27}H_{22}O_6$ -PWAu: C, 37.96; H, 2.60; O, 11.24. Found: C, 37.81; H, 2.45; O, 11.38.

**Spectroscopic data for 6:**  $^1H$  NMR (600 MHz,  $CD_2Cl_2$ , 298 K)  $\delta$  1.25 (t,  $^3J_{H-H} = 7.0$  Hz, 3H, CH<sub>3</sub>), 3.76 (br s, 1H, *cis*-C=CH<sub>2</sub>), 3.92 (q,  $^3J_{H-H} = 7.0$  Hz, 2H, OCH<sub>2</sub>), 4.64 (d,  $^4J_{trans\ P-H} = 9.4$  Hz, 1H, *trans*-C=CH<sub>2</sub>), 7.4–7.6 (m, 15H, Ph);  $^{13}C\{^1H\}$  NMR (150 MHz,  $CD_2Cl_2$ , 298 K)  $\delta$  15.7 (s, CH<sub>3</sub>), 66.2 (s, OCH<sub>2</sub>), 94.4 (d,  $^3J_{P-C} = 6.7$  Hz, =CH<sub>2</sub>), 129.5 (d,  $^2J_{P-C} = 10.5$  Hz, *ortho*-Ph), 131.1 (d,  $^1J_{P-C} = 49.4$  Hz, *ipso*-Ph), 131.7 (s, *para*-Ph), 134.6 (d,  $^3J_{P-C} = 14.2$  Hz, *meta*-Ph), 202.5 (d,  $^2J_{P-C} = 129.8$  Hz, C–Au);  $^{31}P\{^1H\}$  NMR (121.4 MHz,  $CD_2Cl_2$ , 298 K)  $\delta$  42.9 (s, PPh<sub>3</sub>); positive ion FAB-MS  $m/z$  530 ( $M^+$ ). Anal. Calcd for  $C_{22}H_{22}OPAu$ : C, 49.82; H, 4.18; O, 3.02. Found: C, 50.03; H, 4.25; O, 2.88.

**Acknowledgment.** We thank the NRF and the Volkswagen-Stiftung for financial support. The measurement of NMR spectra by the late H. S. C. Spies and E. Marais and the collection of X-ray diffraction data for **1** and **4** by J. Bacsá are gratefully acknowledged. The work at Marburg was financially supported by the DFG and the Fonds der Chemischen Industrie.

**Supporting Information Available:** Crystallographic data in CIF format for compounds **1** and **4**. This material is available free of charge via the Internet at <http://pubs.acs.org>.

OM020048G